M&C 2001 Salt Lake City, Utah, USA, September 2001.

FINITE ELEMENT SOLUTIONS OF SECOND-ORDER FORMS OF THE TRANSPORT EQUATION AT THE INTERFACE BETWEEN DIFFUSIVE AND NON-DIFFUSIVE REGIONS

Christopher J. Gesh
Pacific Northwest National Laboratory
Materials and Engineering Analysis Group, MS K8-34
Richland, Washington 99352
gesh@pnl.gov

Marvin L. Adams
Texas A&M University
Department of Nuclear Engineering
College Station, Texas 77843
mladams@tamu.edu

Keywords: Transport Theory, Even- and Odd-Parity Equations, Asymptotic Analysis

ABSTRACT

We analyze the behavior of even- and odd-parity finite element discretizations of the transport equation at the interface between a diffusive and non-diffusive region in slab geometry. We find that the parity solutions each satisfy interface conditions that may not be accurate, but that their average should be extremely accurate. We discuss and present a self-adjoint angular flux (SAAF) equation boundary condition that makes the SAAF solution identical to the average of separate even- and odd-parity solutions. We conclude with numerical results that agree our analysis predictions.

1 INTRODUCTION

While there has been considerable attention paid to numerical transport solutions inside diffusive regions, relatively little effort has focused on how the solution in a diffusive region affects other portions of the problem. In this paper, we study the behavior of several transport discretizations at the interface between adjacent diffusive and non-diffusive regions.

Recent work (Adams, 1991c, Adams, 1991b, Adams, 1991a, Gesh, 1999b) on finite element method (FEM) discretizations of the even- and odd-parity equations has demonstrated that they possess several desirable properties when applied to problems containing optically thick, diffusive regions. First, these discretizations satisfy corresponding finite element discretizations of the diffusion equation, albeit with potentially inaccurate boundary conditions. Second, the construction of fully consistent diffusion synthetic acceleration (Larsen, 1984) schemes for these discretizations is straightforward.

Recall that the leading order solution of the analytic transport equation satisfies the diffusion equation in the diffusion limit. The associated boundary condition for an incoming angular flux, $f(\mathbf{r},\Omega)$, that produces the correct interior magnitude is given by:

$$\Phi^{[0]}(\mathbf{r}) = 2 \int_{\mathbf{n}\cdot\Omega<0} W(|\mathbf{n}\cdot\Omega|)\, f(\mathbf{r},\Omega)\, d\Omega \quad \text{for } \mathbf{r}\in\partial\mathbf{D}. \tag{1}$$

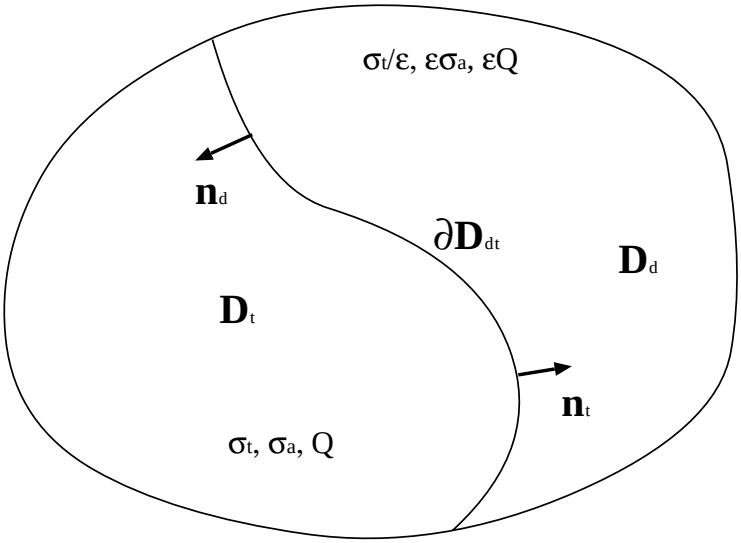

Figure 1: An arbitrary spatial domain with an internal interface.

$W(|\mathbf{n}\cdot\Omega|)$ is defined in terms of Chandrasekhar's H-function and is well approximated by a simple polynomial:

$$W(|\mathbf{n}\cdot\Omega|) = \frac{\sqrt{3}}{2}|\mathbf{n}\cdot\Omega|H(|\mathbf{n}\cdot\Omega|) \simeq |\mathbf{n}\cdot\Omega| + \frac{3}{2}|\mathbf{n}\cdot\Omega|^2. \tag{2}$$

In general, FEM discretizations of the even-parity equation satisfy a $2|\mathbf{n}\cdot\Omega|$ weighted boundary condition, while FEM discretizations of the odd-parity equations satisfy a $3|\mathbf{n}\cdot\Omega|^2$ weighted boundary condition. Thus, the average of the even- and odd-parity FEM solutions should be a very good approximation to the exact solution, as long as the underlying weight and basis functions are carefully chosen. We refer to this average as the *hybrid-parity* method. Similar behavior has been observed for certain reactor physics problems (Ackroyd, 1991).

Here, we restrict our analysis to lumped linear continuous finite element method (LCFEM) discretizations in slab geometry. Fortunately, a great deal of insight can be gained through such analyses because many of the important features of internal interface problems are predominately one-dimensional. We also note that the even-parity continuous FEM system has been analyzed previously for problems like this in three-dimensional geometry with unspecified weight and basis functions (Adams, 1991c). However, there is an minor error in that analysis that invalidates a portion of the results.

2 ANALYTIC DIFFUSION LIMIT ANALYSIS RESULTS

We begin by considering the behavior of the analytic transport equation for an idealized problem containing adjacent diffusive and non-diffusive regions as shown in Fig. 1. This analysis was originally performed by Adams (Adams, 1991c). We denote the boundary between the two regions as $\partial\mathbf{D}_{dt}$ with a normal $\mathbf{n}_d$ that points out of the diffusive region and into the transport region. We also define $\mathbf{n}_t$ as $-\mathbf{n}_d$, so that it points out of the transport region and into the diffusive region.

First, we apply the standard diffusion scaling ($\sigma_t \rightarrow \frac{\sigma_t}{\varepsilon}, \sigma_a \rightarrow \varepsilon\sigma_a$ and $Q \rightarrow \varepsilon Q$) to the

diffusive portion of the problem. We find that:

$$\Psi^{[0]} = \frac{\Phi^{[0]}}{4\pi} \quad \text{for } \mathbf{r} \in \mathbf{D}_d, \tag{3a}$$

$$-\nabla \cdot \frac{1}{3\sigma_t} \nabla \Phi^{[0]} + \sigma_a \Phi^{[0]} = Q \quad \text{for } \mathbf{r} \in \mathbf{D}_d, \tag{3b}$$

and

$$\Phi^{[0]}(\mathbf{r}) = 2 \int\limits_{\mathbf{n}_d \cdot \Omega < 0} W(|\mathbf{n}_d \cdot \Omega|) \Psi^{[0]}(\mathbf{r}, \Omega)\, d\Omega \quad \text{for } \mathbf{r} \in \partial \mathbf{D}_{dt}. \tag{3c}$$

In this expression, $\Psi^{[0]}(\mathbf{r}, \Omega)$ is the as yet unknown angular flux leaving the transport region and entering the diffusive region. Now, we consider the transport region. Obviously, the leading order solution satisfies only the transport equation. The development of the boundary condition is more involved. Here we must determine the value of the angular flux entering $\mathbf{D}_t$ through $\partial \mathbf{D}_{dt}$ as a function of the flux leaving $\mathbf{D}_t$ through $\partial \mathbf{D}_{dt}$. This is corresponds to the problem of determining the albedo of a half-space, which has been solved analytically (Case, 1967). Therefore we have:

$$\Omega \cdot \nabla \Psi^{[0]} + \sigma_t \Psi^{[0]} = \frac{\sigma_t \Phi^{[0]} + Q}{4\pi}, \tag{4a}$$

subject to an albedo condition for $\mathbf{r} \in \partial \mathbf{D}_{dt}$ and $\mathbf{n}_t \cdot \Omega < 0$:

$$\Psi^{[0]}(\mathbf{r}, \Omega) = \frac{1}{2\pi} \int\limits_{\mathbf{n}_t \cdot \Omega' > 0} \alpha(\mu, \mu') \Psi^{[0]}(\mathbf{r}, \Omega')\, d\Omega' \quad \text{where } \mu = |\mathbf{n}_t \cdot \Omega|. \tag{4b}$$

The albedo, $\alpha(\mu, \mu')$, is given by:

$$\alpha(\mu, \mu') = \Big[\frac{W(\mu')}{\mu + \mu'}\Big] \Big/ \Big[\int\limits_0^1 \frac{W(y)}{y + \mu} dy\Big] \quad \text{where } 0 \le \mu, \mu' \le 1. \tag{5}$$

$W(\mu)$ is the weight function shown in equation (2). Note that the albedo interface condition is a function of both the incoming and outgoing angle.

3 SLAB GEOMETRY LUMPED LCFEM EQUATIONS

The even-parity equation and its boundary condition are given by (Lewis, 1984):

$$-\Omega \cdot \nabla \frac{1}{\sigma_t} \Omega \cdot \nabla \Psi^{+} + \sigma_t \Psi^{+} = \frac{\sigma_s \Phi + Q}{4\pi}, \tag{6a}$$

$$(\mathbf{n} \cdot \Omega) \Big(\frac{1}{\sigma_t} \Omega \cdot \nabla \Psi^{+} \Big) = -|\mathbf{n} \cdot \Omega| \Big(\Psi^{+} - f^{+} \Big) \quad \text{for } \mathbf{r} \in \partial \mathbf{D}, \tag{6b}$$

and the odd-parity equation and its boundary condition are:

$$-\Omega \cdot \nabla \frac{1}{\sigma_t} \Omega \cdot \nabla \Psi^{-} + \sigma_t \Psi^{-} = \Omega \cdot \nabla \Big(\frac{\sigma_s \Phi + Q}{4\pi \sigma_t} \Big), \tag{7a}$$

$$\nabla \cdot \Big(2 \int\limits_{2\pi} \Omega \Psi^{-}\, d\Omega \Big) + \sigma_t \Phi = \sigma_s \Phi + Q, \tag{7b}$$

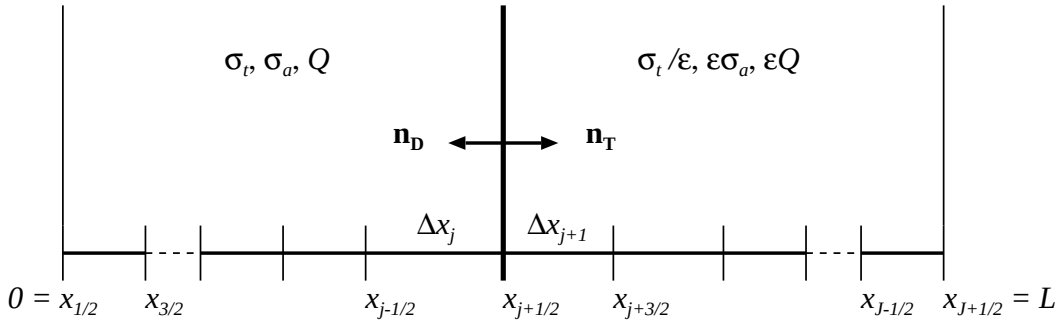

Figure 2: Slab geometry spatial mesh with an internal interface.

$$(\mathbf{n}\cdot\Omega)\Big(\frac{1}{\sigma_t}\Omega\cdot\nabla\Psi^- - \frac{\sigma_s\Phi+Q}{4\pi\sigma_t}\Big) = -|\mathbf{n}\cdot\Omega|(\Psi^- - f^-) \quad \text{for } \mathbf{r}\in\partial\mathbf{D}. \tag{7c}$$

Here, $f^{+/-}$ are the even and odd angular extensions of the incoming angular flux.

We now apply the standard weighted residual method and mass (collision) matrix lumping to the slab geometry forms of equations (6) and (7). In the problem interior, the lumped LCFEM even-parity system is given by:

$$-\mu^2\Big(\frac{\psi^+_{j+3/2}-\psi^+_{j+1/2}}{\sigma_{tj+1}\Delta x_{j+1}} - \frac{\psi^+_{j+1/2}-\psi^+_{j-1/2}}{\sigma_{tj}\Delta x_j}\Big) + \Big(\frac{\sigma_{tj}\Delta x_j+\sigma_{tj+1}\Delta x_{j+1}}{2}\Big)\psi^+_{j+1/2} = \Big(\frac{\sigma_{sj}\Delta x_j+\sigma_{sj+1}\Delta x_{j+1}}{4}\Big)\phi^+_{j+1/2} + \Big(\frac{\Delta x_j+\Delta x_{j+1}}{4}\Big)q^+_{j+1/2} \quad \text{for } j=2..J-1. \tag{8}$$

These equations form a symmetric positive-definite (SPD) matrix problem for each angle. The even-parity scalar flux is linear and continuous in space and can be thought to exist at cell-edges.

The lumped LCFEM odd-parity system is:

$$-\mu^2\Big(\frac{\psi^-_{j+3/2}-\psi^-_{j+1/2}}{\sigma_{tj+1}\Delta x_{j+1}} - \frac{\psi^-_{j+1/2}-\psi^-_{j-1/2}}{\sigma_{tj}\Delta x_{tj}}\Big) + \Big(\frac{\sigma_{tj}\Delta x_j+\sigma_{tj+1}\Delta x_{j+1}}{2}\Big)\psi^-_{j+1/2} = -\frac{\mu}{2}\Big(\frac{\sigma_{sj+1}\phi^-_{j+1}+q^-_{j+1}}{\sigma_{tj+1}} - \frac{\sigma_{sj}\phi^-_j+q^-_j}{\sigma_{tj}}\Big) \quad \text{for } j=2..J-1. \tag{9}$$

$$2\int_0^1 \mu(\psi^-_{j+1/2}-\psi^-_{j-1/2})\,d\mu + \sigma_{tj}\Delta x_j\phi^-_j = \Delta x_j(\sigma_{sj}\phi^-_j+q^-_j) \quad \text{for } j=1..J. \tag{10}$$

The lumped odd-parity system consists of a SPD matrix problem for each angle coupled to cell-centered balance equations. In this case, the odd-parity scalar flux is piecewise constant and can be thought to exist at cell-centers. Note that the hybrid-parity scalar flux for this discretization is piecewise linear-discontinuous in space.

4 INTERNAL INTERFACE ANALYSIS

Consider the spatial mesh shown in Fig. 2. The problem consists of a *non-diffusive* region to the left of $x_{j+1/2}$ and a *diffusive* region to the right of $x_{j+1/2}$. The unscaled transport equation

holds in cells 1 to j (of course, it also holds throughout the entire problem). The diffusion limit results from previous studies (Gesh, 1999b) hold for the cells to the right of, but not including, cell $j+1$. Thus, our task is to find the leading order solution to the discretized transport equation in the two cells immediately adjacent to the interface, that is cells j and $j+1$.

First, we determine the magnitude of the scalar flux on the interface assuming the angular flux incident on the diffusive region from the transport region is known. We then find the angular flux that exits from the diffusive region back into the transport region.

4.1 Even-Parity

At the interface, the scaled even-parity lumped LCFEM equation is:

$$-\mu^2\Big(\varepsilon\frac{\psi^+_{j+3/2}-\psi^+_{j+1/2}}{\sigma_{tj+1}\Delta x_{j+1}}-\frac{\psi^+_{j+1/2}-\psi^+_{j-1/2}}{\sigma_{tj}\Delta x_j}\Big) + \Big(\frac{\sigma_{tj}\Delta x_j}{2}+\frac{\sigma_{tj+1}\Delta x_{j+1}}{2\varepsilon}\Big)\psi^+_{j+1/2} = \frac{1}{4}\Big[\sigma_{sj}\Delta x_j+(\frac{\sigma_{tj+1}}{\varepsilon}-\varepsilon\sigma_{aj+1})\Delta x_{j+1}\Big]\phi^+_{j+1/2} + \Big(\frac{\Delta x_j}{4}+\frac{\varepsilon\Delta x_{j+1}}{4}\Big)q^+_{j+1/2}. \quad (11)$$

The O($1/\varepsilon$) equation shows that the leading order even-parity angular flux is isotropic on the interface between the diffusive and non-diffusive regions:

$$\psi^{+[0]}_{j+1/2}=\frac{1}{2}\phi^{+[0]}_{j+1/2}. \quad (12)$$

The O(1) terms are:

$$\mu^2\Big(\frac{\psi^{+[0]}_{j+1/2}-\psi^{+[0]}_{j-1/2}}{\sigma_{tj}\Delta x_j}\Big)+\frac{\sigma_{tj}\Delta x_j}{2}\psi^{+[0]}_{j+1/2}+\frac{\sigma_{tj+1}\Delta x_{j+1}}{2}\psi^{+[1]}_{j+1/2} = \frac{\sigma_{sj}\Delta x_j}{4}\phi^{+[0]}_{j+1/2}+\frac{\sigma_{tj+1}\Delta x_{j+1}}{4}\phi^{+[1]}_{j+1/2}+\frac{\Delta x_j}{4}q^+_{j+1/2}. \quad (13)$$

The zeroth moment of equation (13) produces:

$$\int_{-1}^{1}\frac{\mu^2}{\sigma_{tj}}\Big(\frac{\psi^{+[0]}_{j+1/2}-\psi^{+[0]}_{j-1/2}}{\Delta x_j}\Big)\,d\mu+\frac{\sigma_{aj}\Delta x_j}{2}\phi^{+[0]}_{j+1/2}=\frac{\Delta x_j}{2}q^+_{j+1/2}. \quad (14)$$

The first term in even in angle, so we can write:

$$\int_{0}^{1}2\frac{\mu^2}{\sigma_{tj}}\Big(\frac{\psi^{+[0]}_{j+1/2}-\psi^{+[0]}_{j-1/2}}{\Delta x_j}\Big)\,d\mu+\frac{\sigma_{aj}\Delta x_j}{2}\phi^{+[0]}_{j+1/2}=\frac{\Delta x_j}{2}q^+_{j+1/2}. \quad (15)$$

We now add and subtract $2\int_0^1 \mu\psi_{j+1/2}^{+[0]} d\mu$ to obtain:

$$-\int_0^1 2\mu\left(\psi_{j+1/2}^{+[0]} - \frac{\mu}{\sigma_{tj}}\frac{\psi_{j+1/2}^{+[0]} - \psi_{j-1/2}^{+[0]}}{\Delta x_j}\right) d\mu + 2\int_0^1 \mu\psi_{j+1/2}^{+[0]} d\mu + \frac{\sigma_{aj}\Delta x_j}{2}\phi_{j+1/2}^{+[0]} = \frac{\Delta x_j}{2} q_{j+1/2}^{+}. \quad (16)$$

Thus, we find that:

$$\phi_{j+1/2}^{+[0]} = \frac{2\int_0^1 2\mu\left(\psi_{j+1/2}^{+[0]} - \frac{\mu}{\sigma_{tj}}\frac{\psi_{j+1/2}^{+[0]} - \psi_{j-1/2}^{+[0]}}{\Delta x_j}\right) d\mu + \Delta x_j q_{j+1/2}^{+}}{1 + \sigma_{aj}\Delta x_j} \quad (17)$$

However, if we assume that the transport region is finely zoned ($\Delta x_j \to 0$), then,

$$\frac{\psi_{j+1/2}^{+[0]} - \psi_{j-1/2}^{+[0]}}{\Delta x_j} \to \left.\frac{d\psi^{+[0]}}{dx}\right|_j. \quad (18)$$

We then identify,

$$\psi_{j+1/2}^{e[0]} = \psi_{j+1/2}^{+[0]} - \frac{\mu}{\sigma_{tj}}\left.\frac{d\psi^{+[0]}}{dx}\right|_j,$$

as the even-parity approximation to the full range angular flux. Thus:

$$\phi_{j+1/2}^{+[0]} = 2\int_0^1 2\mu\psi_{j+1/2}^{e[0]}\, d\mu. \quad (19)$$

That is, the scalar flux on the interface is simply a Marshak weighting of $\psi_{j+1/2}^{e[0]}$, the even-parity approximation to the full range angular flux on the interface.

Now, we must determine what returns from the diffusive region back into the transport region. Recall that the exact solution satisfies the albedo condition shown in equation (5). Our goal here is to find the corresponding albedo for the discrete even-parity system.

It is straightforward to show that at a boundary for $\mu < 0$:

$$\psi^e(x_b, \mu) = 2\psi^+(x_b, \mu) - f(x_b, -\mu),$$

where $f(x_b, -\mu)$ is the angular flux incident upon that boundary. We have just shown in equation (12) that the even-parity angular flux on the interface between the diffusive and non-diffusive

region is isotropic. Using equations (12) and (19), we find that for $\mu < 0$:

$$\begin{aligned}
\psi^{e[0]}_{j+1/2}(\mu) &= 2\psi^{+[0]}_{j+1/2}(\mu) - f(-\mu) \qquad (20a)\\
&= \phi^{+[0]}_{j+1/2} - \psi^{e[0]}_{j+1/2}(-\mu)\\
&= 2\int_0^1 2\mu'\psi^{e[0]}_{j+1/2}(\mu')\,d\mu' - \psi^{e[0]}_{j+1/2}(-\mu)\\
&= \int_0^1 \alpha^e(\mu,\mu')\psi^{e[0]}_{j+1/2}(\mu')\,d\mu'
\end{aligned}$$

where we have defined the albedo, $\alpha^e(\mu,\mu')$, as:

$$\alpha^e(\mu,\mu') = 4\mu' - \delta(\mu'+\mu). \qquad (20b)$$

We have also identified $f(-\mu)$ as $\psi^{e[0]}_{j+1/2}(-\mu)$, which is appropriate for the albedo problem we are considering. To summarize, we can now say that the leading order even-parity solution in a problem with an internal interface satisfies:

- the discrete even-parity transport equation for all the cells from the left boundary to the interface, subject to the albedo interface condition shown in equation (20), and
- the discrete diffusion limit even-parity system for all the cells from the interface to the right boundary, subject to weighted interface condition shown in equation (19).

4.2 Odd-Parity

At the interface, the scaled odd-parity lumped LCFEM equations are:

$$\begin{aligned}
-\mu^2\Big(\varepsilon\frac{\psi^-_{j+3/2}-\psi^-_{j+1/2}}{\sigma_{tj+1}\Delta x_{j+1}} - \frac{\psi^-_{j+1/2}-\psi^-_{j-1/2}}{\sigma_{tj}\Delta x_{tj}}\Big) + \Big(\frac{\sigma_{tj}\Delta x_j}{2} + \frac{\sigma_{tj+1}\Delta x_{j+1}}{2\varepsilon}\Big)\psi^-_{j+1/2}&\\
= -\frac{\mu}{2}\Big(\frac{(\sigma_{tj+1}-\varepsilon^2\sigma_{aj+1})\phi^-_{j+1}+\varepsilon^2 q^-_{j+1}}{\sigma_{tj+1}} - \frac{\sigma_{sj}\phi^-_j + q^-_j}{\sigma_{tj}}\Big), \qquad (21a)&
\end{aligned}$$

$$2\int_0^1 \mu(\psi^-_{j+1/2}-\psi^-_{j-1/2})\,d\mu + \sigma_{aj}\Delta x_j\phi^-_j = \Delta x_j q^-_j, \qquad (21b)$$

$$2\int_0^1 \mu(\psi^-_{j+3/2}-\psi^-_{j+1/2})\,d\mu + \varepsilon\sigma_{aj+1}\Delta x_{j+1}\phi^-_{j+1} = \varepsilon\Delta x_{j+1}q^-_{j+1}. \qquad (21c)$$

The O$(1/\varepsilon)$ equation shows that the leading order odd-parity angular flux is zero:

$$\psi^{-[0]}_{j+1/2} = 0. \qquad (22)$$

The O(1) terms of equation (21a) are:

$$\mu^2\Big(\frac{\psi^{-[0]}_{j+1/2}-\psi^{-[0]}_{j-1/2}}{\sigma_{tj}\Delta x_{tj}}\Big) + \frac{\sigma_{tj+1}\Delta x_{j+1}}{2}\psi^{-[1]}_{j+1/2} = -\frac{\mu}{2}\Big(\phi^{-[0]}_{j+1} - \frac{\sigma_{sj}\phi^{-[0]}_j + q^-_j}{\sigma_{tj}}\Big), \qquad (23)$$

where we have used the O$(1/\varepsilon)$ result in the collision term, but not in the leakage term. We solve for $\psi^{-[1]}_{j+1/2}$ and take the μ moment to find:

$$\frac{\sigma_{tj+1}\Delta x_{j+1}}{2}\int_{-1}^{1}\mu\psi^{-[1]}_{j+1/2}\,d\mu$$
$$= -\frac{1}{3}\phi^{-[0]}_{j+1} + \int_0^1 2\mu^2\Big(-\mu\frac{\psi^{-[0]}_{j+1/2}-\psi^{-[0]}_{j-1/2}}{\sigma_{tj}\Delta x_{tj}} + \frac{\sigma_{sj}\phi^{-[0]}_j + q^-_j}{2\sigma_{tj}}\Big)\,d\mu. \quad (24)$$

If we again assume that the transport region is finely zoned ($\Delta x_j \to 0$), then,

$$\frac{\psi^{-[0]}_{j+1/2}-\psi^{-[0]}_{j-1/2}}{\Delta x_j} \to \left.\frac{d\psi^{-[0]}}{dx}\right|_j. \quad (25)$$

Also, we know that the odd-parity approximation to the full range angular flux, ψ^o, is given by:

$$\psi^{o[0]}_{j+1/2} = \psi^{-[0]}_{j+1/2} - \frac{\mu}{\sigma_{tj}}\left.\frac{d\psi^{-[0]}}{dx}\right|_j + \frac{\sigma_{sj}\phi^{-[0]}_j + q^-_j}{2\sigma_{tj}}.$$

Since the term in parenthesis in equation (24) is just $\psi^{o[0]}_{j+1/2}$, and the leading order odd-parity angular flux is zero, we have:

$$\int_{-1}^{1}\mu\psi^{-[1]}_{j+1/2}\,d\mu = -\frac{1}{3}\frac{\phi^{-[0]}_{j+1} - 2\int_0^1 3\mu^2\psi^{o[0]}_{j+1/2}\,d\mu}{(\sigma_{tj+1}\Delta x_{j+1}/2)}. \quad (26)$$

Finally, we use the above result and take the zeroth moment of the O(1) terms in equation (21c) to obtain:

$$-\frac{1}{3}\Big[\frac{\phi^{-[0]}_{j+2}-\phi^{-[0]}_{j+1}}{(\sigma_{tj+2}\Delta x_{j+2}+\sigma_{tj+1}\Delta x_{j+1})/2} - \frac{\phi^{-[0]}_{j+1}-\phi^{-[0]}_{j+1/2}}{(\sigma_{tj+1}\Delta x_{j+1}/2)}\Big] + \sigma_{aj+1}\Delta x_{j+1}\phi^{-[0]}_{j+1}$$
$$= \Delta x_{j+1}q^-_{j+1}, \quad (27a)$$

where,

$$\phi^{-[0]}_{j+1/2} = 2\int_0^1 3\mu^2\psi^{o[0]}_{j+1/2}\,d\mu. \quad (27b)$$

We have used the interior analysis results to evaluate the μ moment of $\psi^{-[1]}_{j+3/2}$. Thus, the boundary condition for the leading order scalar flux in the diffusive region is the $3\mu^2$ moment of the odd-parity approximation to the incident flux from the transport region.

Now, we must find the angular flux that returns from the diffusive region back into the transport region. At a boundary for $\mu < 0$ we can write:

$$\psi^o(x_b,\mu) = 2\psi^-(x_b,\mu) + f(x_b,-\mu),$$

The leading order odd-parity angular flux on the interface between the diffusive and transport region

is zero; thus for $\mu < 0$:

$$\begin{aligned} \psi^{o[0]}_{j+1/2}(\mu) &= f(-\mu) \\ &= \psi^{o[0]}_{j+1/2}(-\mu) \\ &= \int_0^1 \alpha^o(\mu,\mu')\psi^{o[0]}_{j+1/2}(\mu')\,d\mu' \end{aligned} \tag{28a}$$

where we have defined the albedo, $\alpha^o(\mu,\mu')$, as:

$$\alpha^o(\mu,\mu') = \delta(\mu'+\mu). \tag{28b}$$

To summarize, we can now say that the leading order odd-parity solution in a problem with an internal interface satisfies:

- the discrete odd-parity transport system for all the cells from the left boundary to the interface, subject to albedo boundary condition shown in equation (28), and
- the discrete diffusion limit odd-parity system for all the cells from the interface to the right boundary, subject to equation (27b).

4.3 Hybrid-Parity

Just as in an entirely diffusive problem, it appears that the average of the even- and odd-parity solutions results in the correct weighted interface condition for the diffusive portion of the problem. Specifically,

$$\frac{\phi^{-[0]}_{j+1/2} + \phi^{+[0]}_{j+1/2}}{2} = 2\Big(\int_0^1 \mu\psi^{e[0]}_{j+1/2}\,d\mu + \int_0^1 \frac{3}{2}\mu^2\psi^{o[0]}_{j+1/2}\,d\mu\Big).$$

If the transport region is zoned finely enough to resolve the solution in both the even- and odd-parity cases,

$$\psi^{e[0]}_{j+1/2}(\mu) \simeq \psi^{o[0]}_{j+1/2}(\mu) \simeq \psi^{[0]}_{j+1/2}(\mu) \tag{29}$$

then we have,

$$\frac{\phi^{-[0]}_{j+1/2} + \phi^{+[0]}_{j+1/2}}{2} = 2\int_0^1 (\mu + \frac{3}{2}\mu^2)\psi^{[0]}_{j+1/2}\,d\mu. \tag{30}$$

This is a highly desirable result. Again, we see that the average of the parity scalar fluxes should be very accurate for diffusive portions of the problem, assuming that the transport portions are zoned finely enough so that equation (29) holds.

A more difficult question to answer is whether or not the average of the even- and odd-parity solutions results in the correct angular flux returning into the transport region. Let us consider the average of the parity albedo conditions. We have:

$$\frac{\alpha^e(\mu,\mu') + \alpha^o(\mu,\mu')}{2} = \frac{1}{2}\Big[4\mu' - \delta(\mu'+\mu) + \delta(\mu'+\mu)\Big] = 2\mu'. \tag{31}$$

This is an interesting result for two reasons. First, we see that this albedo is not a function of returning angle. The particles returning back into the transport region are isotropically distributed

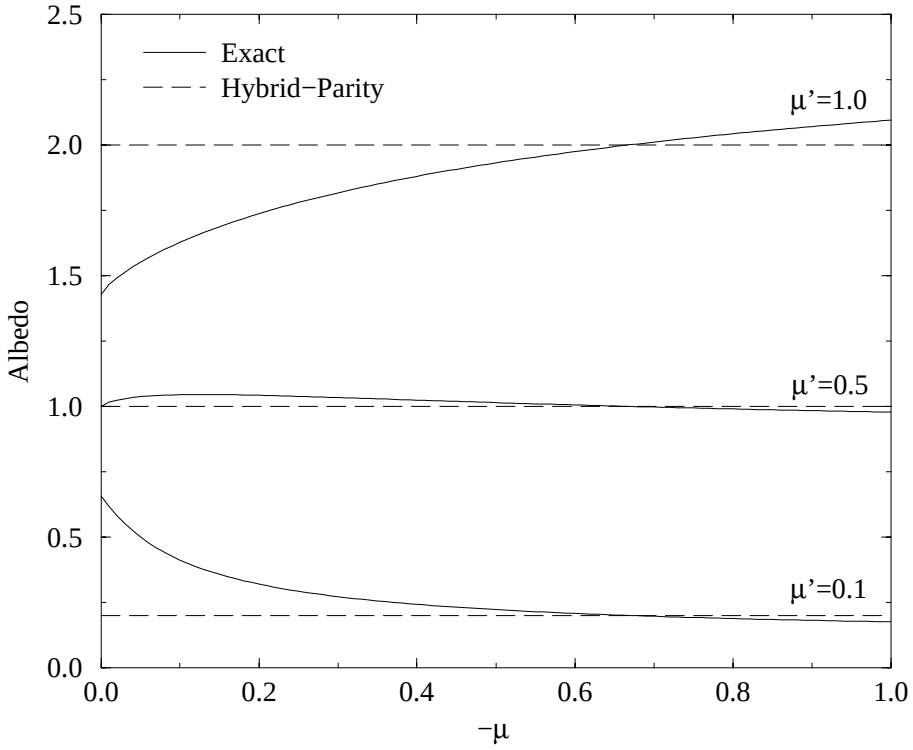

Figure 3: Exact and hybrid-parity albedo weighting functions.

in angle. Second, particles are conserved by the μ' weighting of the incoming angular flux.

The exact albedo boundary, however, not only conserves particles but also returns particles back into the transport region anisotropically. In Fig. 3 we plot the exact albedo and the hybrid-parity albedo for various values of μ' as a function of the returning angle. We see from the figure that the largest discrepancies occur for small angles, which have the least impact on the returning solution. In the numerical results section, we verify this behavior and show that the average of the even- and odd-parity solutions is indeed very accurate for problems of this type.

4.4 SAAF

It has been shown that the LCFEM self-adjoint angular flux (SAAF) equations (Morel, 1999) are identical to the average of the even- and odd-parity equations in the problem interior, though they differ at external boundaries (Gesh, 1999a). Thus, our simple analysis of the hybrid-parity method applies directly to the SAAF LCFEM system. The leading order solutions satisfy the same discrete equations in the problem interior.

As we mentioned, however, they may satisfy different exterior boundary conditions. If we use the standard SAAF boundary condition (which is incorporated naturally into the LCFEM system):

$$\psi_b(\mathbf{r},\Omega) = f(\mathbf{r},\Omega) \quad \text{for } \mathbf{n}\cdot\Omega < 0, \tag{32}$$

then we do not expect the SAAF solutions to exactly agree with the parity solutions. If, on the other hand, we use:

$$\psi_b(\mathbf{r},\Omega) = 2f(\mathbf{r},\Omega) - \psi(\mathbf{r},\Omega) \quad \text{for } \mathbf{n}\cdot\Omega < 0 \tag{33}$$

then we expect exact agreement (Gesh, 1999a). We verify this in the numerical results section.

This behavior is interesting. Using the standard SAAF boundary condition, the cell-centered unknowns satisfy a $\mu + \frac{3}{2}\mu^2$ weighting on exterior boundaries, which makes the use of the cell-centered fluxes appealing for diffusive problems. Unfortunately, the cell-centered unknowns satisfy a $3\mu^2$ interface condition on internal interfaces. If we were to replace the standard SAAF boundary condition with equation (33), we would expect the cell-centered unknowns to satisfy a $3\mu^2$ weighting on exterior boundaries and on internal interfaces. Note that the cell-edge unknowns satisfy a 2μ weighting on exterior boundaries and on internal interfaces for *both* forms of the SAAF boundary condition. Thus, the average of cell-centered and cell edge unknowns from a SAAF calculation using equation (33) will satisfy a $\mu + \frac{3}{2}\mu^2$ weighted boundary condition on both external boundaries and internal interfaces. It is, obviously, identical to the hybrid parity result. Using the standard SAAF boundary condition will result in very accurate cell-centered fluxes for problems that are entirely diffusive. However, the cell-centered results may not be accurate for problems with internal interfaces. It is very interesting, and perhaps counter-intuitive, that a change in the *outer* boundary condition has such a dramatic effect on the SAAF solution at an *internal interface*.

5 NUMERICAL RESULTS

We now consider a model internal interface problem. This problem consists of a two-region slab. The first region ($0 < x < 1.0$) contains a source free pure absorber one mean-free path thick. The second region ($1.0 < x < 2.0$) contains a source-free pure scatterer one thousand mean free paths thick. The problem is driven by an incident angular flux at $x = 0$. All calculations were performed using S_{16} quadrature and the reference results were obtained with diamond difference calculations using 10^3 cells in the transport region and 10^4 cells in the diffusive region.

Recall that the angular flux in the transport region is described by equations (4) and (5). If the transport region consists of a pure absorber, we can analytically calculate the solution in that region. First, we attenuate the external boundary condition from the left boundary to the interface. Then we use the albedo condition, equation (5), to determine the angular flux emerging from the diffusive region and attenuate that from the interface to the left boundary. We note that we use the discrete ordinates method to treat the angle variable, though that is by no means necessary. We simply want the spatially analytic results to correspond as closely as possible to the numerical results.

We also found that the even- and odd-parity systems each satisfied albedo conditions at the interface. These interface albedo conditions, equations (20b) and (28b), significantly differ from the exact condition. However, their average results in a 2μ weighted isotropic return which we think may be an acceptable approximation to the exact condition.

Fig. 4 shows the exact analytic scalar flux in the transport region along with the analytic even- and odd-parity results calculated with equations (20b) and (28b) for an incident angular flux in the most normal direction. We have also plotted even- and odd-parity numerical results for this problem. The numerical results in the transport region agree quite well with the analytic predictions, and the hybrid-parity solution is very accurate for this problem. As we showed in Fig. 3, the hybrid-parity albedo differs from the exact mainly at small values of μ, which influences the overall solution the least.

Now, we consider the model interface problem driven by a left boundary angular flux in the most normal direction. We use 10 cells in the transport region and 10 cells in the diffusive region. The reference solution displays an abrupt jump in magnitude (a boundary layer) at the interface as shown in Fig. 5. Assuming that the transport region is zoned finely enough to resolve the angular flux for $\mu > 0$, we expect the even-parity solution to satisfy a 2μ weighted boundary condition on the interface, and the odd-parity to satisfy a $3\mu^2$ condition. Thus, the even-parity solution should

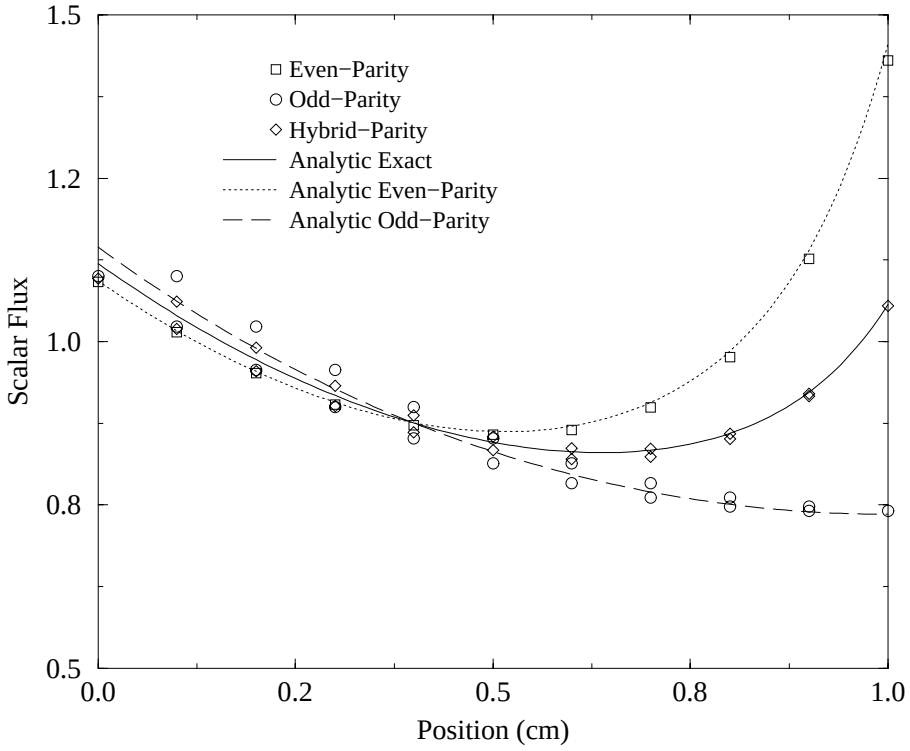

Figure 4: Analytic internal interface solution for $x < 1$.

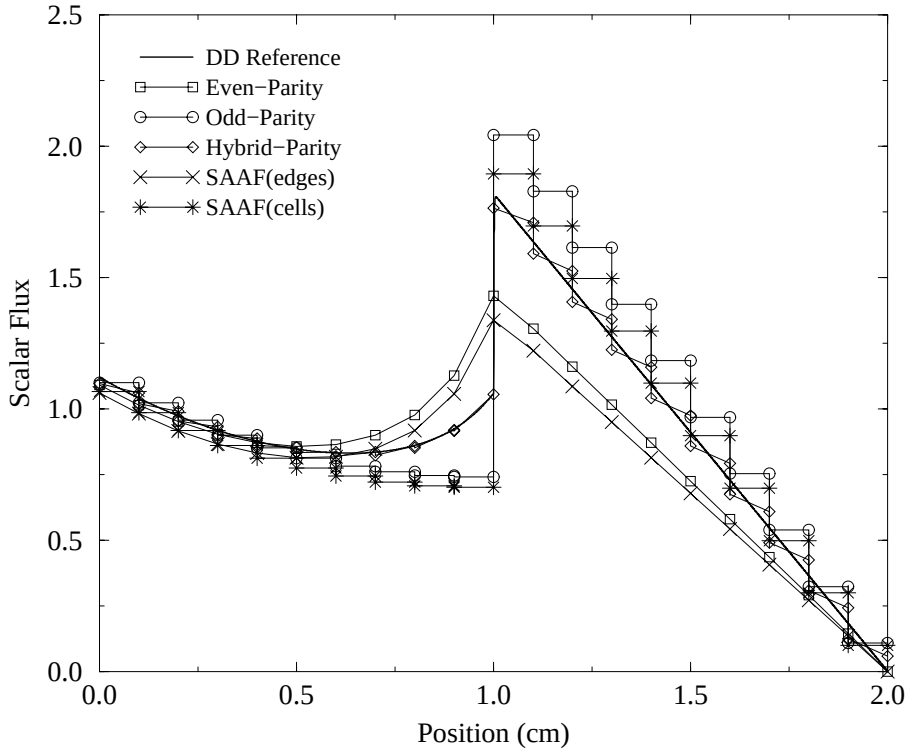

Figure 5: Normal incident flux interface problem.

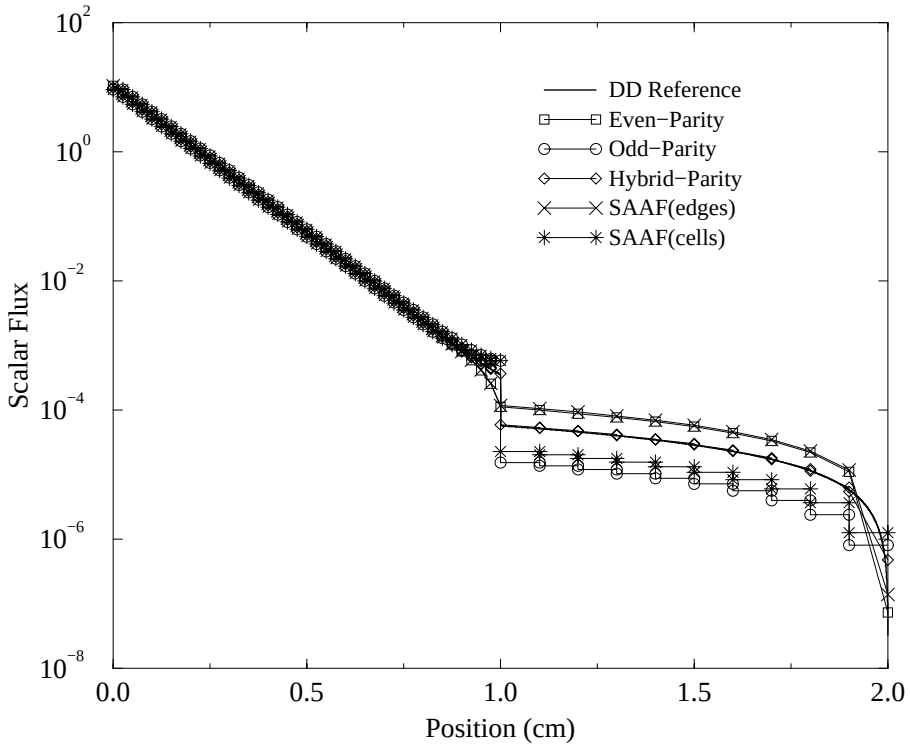

Figure 6: Grazing incident flux interface problem (log scale).

be lower than the exact for $\mu \simeq 1$, and the odd-parity high. That is exactly what we observe. Their average, as predicted, is very accurate in both the transport and diffusive region. Recall that we can formally relate the SAAF solutions to the parity solutions at the interface. That is, we expect the SAAF cell-edge scalar fluxes to be nearly identical to the even-parity values, and the SAAF cell center fluxes to match the odd-parity values. This is very nearly the case and we postulate that the observed differences are a result of the way we treat the external boundary condition.

In Fig. 6 we consider the model problem driven by a grazing incoming angular flux. In this case, we use 100 zones in the transport region and 10 in the diffusive. The larger number of zones in the transport region is required to account for the exponential attenuation of the solution over a longer path length (the distance that a beam must travel to reach the interface is $1/\mu$, thus for small μ more cells are required to resolve the solution). This problem has a strong boundary layer in which the reference solution changes by an order of magnitude. Despite this, the hybrid-parity solution is extremely accurate.

Finally, we plot the SAAF results obtained with the $\psi_b = 2f_l - \psi_{1/2}$ boundary condition in Fig. 7. Here, we expect the SAAF edge scalar fluxes to be identical to the even-parity fluxes, and the SAAF cell fluxes to correspond to the odd-parity fluxes. This is precisely what we observe. Finally, we note that though the standard SAAF boundary condition results in cell-centered scalar fluxes that are correct on the external boundaries of thick diffusive problems, the cell-centered flux is not accurate at internal interfaces. Using the modified boundary condition, the average of the cell-edge and cell-centered SAAF scalar fluxes is extremely accurate at both external boundaries and internal interfaces.

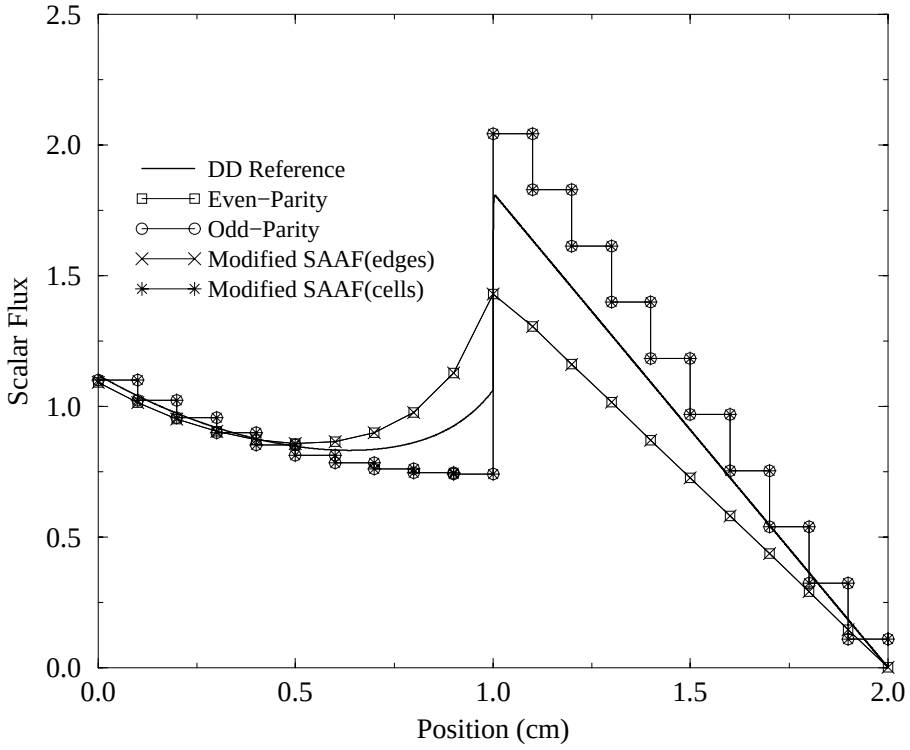

Figure 7: Normal incident modified SAAF interface problem.

6 CONCLUSIONS

We have analyzed the lumped LCFEM even- and odd-parity equations at an internal interface. We have shown that the leading order parity solutions satisfy corresponding finite element discretizations of the diffusion equation in the diffusive region along with weighted interface conditions that may not be accurate. The average of the even- and odd-parity solutions is, however, quite accurate. In the non-diffusive region, the parity solutions satisfy the parity transport equations with albedo interface conditions that can again be inaccurate. However, their average is sufficiently close to exact albedo that both analytic and numerical solutions agree very well with exact and/or reference solutions for a range of model problems. However, the same may not be true for certain realistic multidimensional problems, where solutions can be strongly dependent on the angular shape of the flux emerging from diffusive regions. We stress that for the hybrid-parity solution to be accurate throughout the problem, the zoning in the non-diffusive region must be suffient to resolve the solution there.

Our analysis has also shown that the standard SAAF boundary condition can result in inaccurate cell-centered solutions at internal interfaces despite their excellent behavior in entirely diffusive problems. We presented a modified SAAF boundary condition that effectively makes SAAF system equivalent to the hybrid-parity system. Our numerical results verify this behavior.

REFERENCES

Ackroyd, R. T., Nanneh, M. M., 1991. Hybrid principle with application to synthesis. *Prog. Nucl. Energy* **25**, 199–208.

Adams, M. L., 1991a. Discontinuous finite-element transport solutions in the thick diffusion limit in Cartesian geometry. In: *Proceedings of the International Topical Meeting on Advances in Mathematics, Computations and Reactor Physics*, Pittsburgh, Pennsylvania, The American Nuclear Society, pp. 21.1 (3–1 to 3–12).

Adams, M. L., 1991b. Even- and odd-parity finite-element transport solutions in the thick diffusion limit. In: *Proceedings of the International Topical Meeting on Advances in Mathematics, Computations and Reactor Physics*, Pittsburgh, Pennsylvania, The American Nuclear Society, pp. 21.1 (2–1 to 2–12).

Adams, M. L., 1991c. Even-parity finite-element transport methods in the diffusion limit. *Prog. Nucl. Energy* **25**, 159–197.

Case, K. M., Zweifel, P. M., 1967. *Linear Transport Theory*. Addison-Wesley, Reading, Massachusetts.

Gesh, C. J., 1999a. *Finite Element Methods for Second Order Forms of the Transport Equation*. PhD thesis, Texas A&M University.

Gesh, C. J., Adams, M. L., 1999b. Even- and odd-parity finite element solutions to thick diffusive problems in Cartesian geometry. In: *Proceedings of the International Conference on Mathematics and Computation, Reactor Physics and Enviromental Analysis in Nuclear Applications*, Madrid, Spain, The American Nuclear Society, pp. 1175–1184.

Larsen, E. W., 1984. Diffusion-synthetic acceleration methods for discrete ordinates problems. *Transp. Theory Stat. Phys.* **13**, 107–126.

Lewis, E. E., Miller, Jr., W. F., 1984. *Computational Methods of Neutron Transport*. Wiley, New York.

Morel, J. E., McGhee, J. M., 1999. A self-adjoint angular flux equation. *Nucl. Sci. Eng.* **132**, 312–325.